



Effects of oxygen addition on physical properties of ZnO thin film grown by radio frequency reactive magnetron sputtering

Che-Wei Hsu^a, Tsung-Chieh Cheng^b, Chun-Hui Yang^c, Yi-Ling Shen^c, Jong-Shinn Wu^{a,*}, Sheng-Yao Wu^b

^a Department of Mechanical Engineering, National Chiao Tung University, 1001 Ta-Hsueh Road, Hsinchu 30010, Taiwan

^b Department of Mechanical Engineering, National Kaohsiung University of Applied Science, 415 Chien Kung Road, Kaohsiung 807, Taiwan

^c National Nano Device Laboratories, No. 26, Prosperity Road I, Science-based Industrial Park, Hsinchu 30078, Taiwan

ARTICLE INFO

Article history:

Received 19 May 2010

Received in revised form

28 September 2010

Accepted 13 October 2010

Available online 21 October 2010

Keywords:

Zinc oxide

Radio frequency

Sputtering

Target poisoning

X-ray diffraction

X-ray photoelectron spectroscopy

ABSTRACT

We deposited a ZnO thin film on a microslide glass substrate at room temperature by employing the RF reactive magnetron sputtering process. Our results revealed that deposition rate decreases by increasing $O_2/(Ar + O_2)$ ratio that was caused by two mechanisms. The first mechanism was the reduction of plasma density and, thus, argon ion density; caused by the addition of highly electronegative oxygen. While the second mechanism was target poisoning caused by the oxidation of the target. Additionally, at the $O_2/(Ar + O_2)$ ratio of ~ 0.3 and the help of XPS analysis the optimum stoichiometry of ZnO thin film (the highest binding energy and content fraction of O^1 peak (O–Zn bond)) and the best polycrystallinity (the lowest FWHM with largest grain size) was found.

© 2010 Elsevier B.V. All rights reserved.

1. Introduction

Zinc oxide (ZnO) is an interesting semiconductor II–VI compound material of broad scientific and technological importance. Due to the unique properties of ZnO, the broad application of this compound material in fields such as optoelectronics [1,2], sensors [3], piezoelectric [4], and energy and environment [5,6]. These unique properties of ZnO include a hexagonal wurtzite structure, a wide direct band gap of 3.37 eV at room temperature (RT), a high sensitivity to various gases, a highly piezoelectric coupling coefficient, a highly electrical conductive, and stable chemical and thermal properties; among others.

ZnO films can be deposited by a variety of techniques such as sputtering [7–9], chemical bath deposition, spray pyrolysis, pulsed laser deposition, and metal organic chemical vapor deposition. Among them, the sputtering method represents one of the simplest and most effective methods that can be used to obtain higher thin film orientation and uniformity with low growth temperature, including amorphous substrate. However, the material properties of ZnO thin films are critically related to the plasma deposited tech-

niques and to the growth parameters. Therefore, understanding the relationship between material properties and plasma characteristics should greatly help to produce high-quality ZnO thin film.

In a process similar to that done in other research [7–9], we applied a sputtering technique in order to deposit ZnO thin film for the purpose of investigating the relationship between general plasma properties and general film properties [10]. In addition, the glass substrate was used because it possesses a huge potential market for future applications, such as heat-reflecting coating [5], architectural/low-emissivity windows [6,11–15], and windshield (anti-ultraviolet characteristics). We present the effects of the $O_2/(Ar + O_2)$ ratio on ZnO film properties (crystal structure, orientation, and composition) while focusing on the role of O–Zn bond, which has been largely ignored in previous studies. This said, the influence of oxygen on film properties (crystalline structure, surface morphology, and composition) has been well studied [16–21].

2. Experimental setup

In this study, the ZnO thin film was deposited on a microslide glass substrate at RT with a Zn target. This was performed using the RF reactive magnetron sputtering process, as described in detail in our previous study [10]. Argon and oxygen were used as the major discharge and reactive gases, respectively. Distance between the target and substrate was kept as 8 cm throughout the study. ZnO thin films were grown using a fixed RF power of 100 W and a working pressure of 15 mTorr. The major test conditions for preparing ZnO thin film include maintaining the

* Corresponding author. Tel.: +886 3 573 1693; fax: +886 3 572 0634.

E-mail address: chongsin@faculty.nctu.edu.tw (J.-S. Wu).

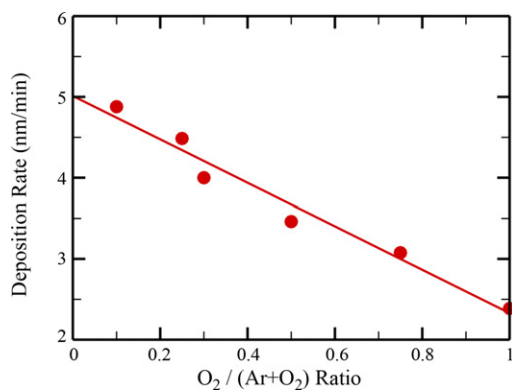


Fig. 1. The deposition rate as a function of $O_2/(Ar+O_2)$ ratio in a plasma used for ZnO thin film deposition.

$O_2/(Ar+O_2)$ ratio ranges between 0.1 and 1.0 while keeping a constant film thickness of 60 nm; the latter is measured by a surface profilometer. The crystal structure and orientation of the films was determined using the X-ray diffraction (XRD) technique. The composition and chemical state of oxygen in the ZnO thin film was studied with an X-ray photoelectron spectroscopy (XPS). All obtained spectra were calibrated to a C1s electron peak at 284.6 eV [16].

3. Results and discussion

3.1. Deposition rate

Fig. 1 illustrates the deposition rate of the ZnO thin film as a function of $O_2/(Ar+O_2)$ ratio through the magnetron sputtering process. In general, the deposition rate decreases monotonically with increasing $O_2/(Ar+O_2)$ ratio. We concluded that there are two possible mechanisms which cause the observed $O_2/(Ar+O_2)$ ratio effect. The first one is that the addition of electronegative oxygen that is highly affinitive to electrons in the discharge reduces the plasma density, which results in fewer electrons, fewer positive argon ions and more negative oxygen ions. In addition, the ionization threshold of oxygen is much higher than of argon [22,23]. Thus, the further addition of oxygen leads to weaker plasma and results in decreasing deposition rate [24]. The second one is caused by the so-called “target poisoning”. This can occur when the target surface is in direct react with oxygen as oxygen is added into the sputtering chamber. This will create a very thin oxide layer on the surface of metal target. Therefore, the target surface may change from metal to ceramic-like ($Zn \rightarrow ZnO_x$). The addition of this oxide layer on the target acts like a dielectric layer which shields the applied voltage (thus, the electric field) that leads to lower ion bombardment energy onto the target. This may further deteriorate as more oxygen is added.

In brief summary, results indicated a reduction in plasma number density and thus the reduction of ion flux/energy in bombarding the target [21,25,26]. Accordingly, this also reduced the sputtering yield, which resulted in a lower deposition rate at a higher $O_2/(Ar+O_2)$ ratio [21,27].

3.2. Structural properties

Fig. 2a shows the XRD data for all combinations of $O_2/(Ar+O_2)$ ratio, while Fig. 2b shows that the FWHM of (0002) as well as estimated grain size (Scherrer equation [23]) as a function of the $O_2/(Ar+O_2)$ ratio. Drawing from the XRD pattern, the deposited ZnO film is a typical poly-crystalline phase with a hexagonal structure and a clear (0002) orientation for the $O_2/(Ar+O_2)$ ratios tested. A minimal value of FWHM was obtained at ~ 0.3 of the $O_2/(Ar+O_2)$ ratio where the corresponding grain size was the largest (35.68 nm). Bachari et al. [17] argued that in the film

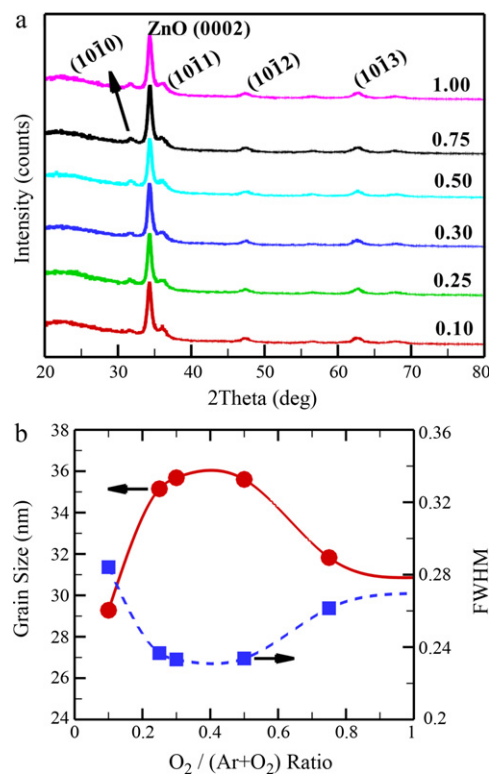


Fig. 2. (a) XRD pattern of ZnO thin film with various $O_2/(Ar+O_2)$ ratios and (b) the FWHM and the calculated grain size as a function of $O_2/(Ar+O_2)$ ratio, respectively.

structure, less oxygen will cause an increase in crystallographic defects while more oxygen will destroy the stoichiometry due to the lower surface mobility of the deposited atoms and lower kinetic energy for surface diffusion. In addition, adding more oxygen into the discharge might produce more neutral oxygen atoms which diffuse into films without low energy [21–23], thus creating additional unexpected defects. Furthermore, grain size increases from 29.28 nm at 0.1 of $O_2/(Ar+O_2)$ ratio up to 35.68 nm at 0.3 of $O_2/(Ar+O_2)$ ratio, and then decreases gradually down to 30.86 nm eventually at 1.0 of $O_2/(Ar+O_2)$ ratio. In other words, the maximum grain size also occurs at 0.3 of $O_2/(Ar+O_2)$ ratio that is consistent with the lowest FWHM of ZnO thin film observed in this study. According to Kajikawa [28] report, the texture of the films should be different when changing the $O_2/(Ar+O_2)$ ratio. However, it was not observed in the current study which is quite different from previous studies in terms of magnetron types [29], sputtering powers, chamber pressures [30] and substrate materials [24]. So far, there was no systematic study that focused on clarifying this observation, which is definitely worthy of further investigation in the future.

3.3. Chemical properties

Fig. 3 presents the XPS analysis results from the deposited ZnO thin films. All specimens revealed that the binding energy of Zn 2p3 peak was about 1021.8 eV [18]. Thus, Zn was not seen to exhibit obvious change in its chemical state over the course of this study. Nevertheless, the chemical state of the O 1s peak showed appreciable shift as illustrated in Fig. 3a. In brief, the binding energy of the O 1s peaks were divided into two components, O^I (the binding energy at 529.8 eV) and O^II (the binding energy at 531.6 eV), respectively. The O^I peak was attributed the presence of O^{2-} ions in the wurtzite ZnO thin films (O–Zn bond), while the O^II peak may have been caused by the loosely bound oxygen created by absorbed H_2O or by the O^{2-} ions in the oxygen deficiency produced on the surface

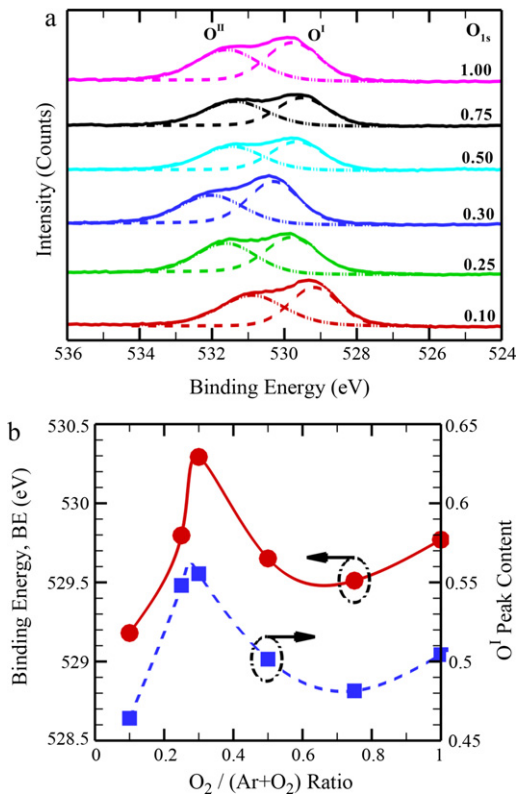


Fig. 3. (a) The O1s spectra (solid line), O' peak (dashed line) and O' peak (dot line) of XPS and (b) the binding energy (●) and the content (■) of O' peak with various $O_2/(Ar + O_2)$ ratio, respectively.

during the ZnO thin film growth (O–H bond or O–O bond) [19,20]. As shown in Fig. 3a, both O' and O' peaks shifted to a higher binding energy with an increasing ratio of $O_2/(Ar + O_2)$ in the range of 0.1–0.3, which had the effect of decreasing the number of defect sites. In contrary, as more oxygen was added to the discharge, more low energy neutral oxygen might diffuse into the growing film, destroying its stoichiometry. These findings are summarized in Fig. 3b, which shows the binding energy and content fraction of O' peak as a function of the $O_2/(Ar + O_2)$ ratio, in which the trend of these two properties correlate very well with each other. In addition, clear maximal values were found at the $O_2/(Ar + O_2)$ ratio of 0.3 coinciding with the minimal value observation of FWHM observed in the XRD analysis (Fig. 2b). These findings reveal that the magnitudes of both the binding energy and content fraction of the O' peak (O–Zn bond) play a key role in the stoichiometry of ZnO film. The above observations suggest that suitable oxygen content can produce ZnO film that is close to stoichiometric. Therefore, we deduce that the optimum stoichiometric and quality of ZnO thin film may be obtained at the $O_2/(Ar + O_2)$ ratio of 0.3 under the current experimental configuration.

4. Conclusion

In our study, a ZnO thin film was successfully deposited on a microslide glass substrate at RT through the employment of RF reactive magnetron sputtering process. The results show that the deposition rate decreases as the $O_2/(Ar + O_2)$ ratio increases

because of two mechanisms. These two mechanisms were the addition of electronegative oxygen and target poisoning. In addition, at the $O_2/(Ar + O_2)$ ratio of ~ 0.3 , with the help of XPS analysis, the optimum stoichiometry of ZnO thin film (the highest binding energy and content fraction of O' peak (O–Zn bond)) and the best polycrystallinity (the lowest FWHM with largest grain size) were found. Our findings showed that appropriate oxygen addition into the discharge is critical in optimizing the ZnO film structure. However, the best quality and stoichiometry of ZnO thin film simultaneously were observed at the $O_2/(Ar + O_2)$ ratio of 0.3 for deposition on glass substrate with the RF power 100 W.

Acknowledgements

The authors would like to express their sincere thanks to the financial support of National Science Council of Taiwan through NSC 96-2628-E-009-134-MY3 and NSC 96-2628-E-009-136-MY3. Also the instrumentation provided by National Nano Device Laboratory of Taiwan is also highly appreciated. The authors are also thankful to Professor T.C. Wei of Department of Chemical Engineering, Chung Yuan Christian University, Taiwan for useful discussion during the preparation of the manuscript.

References

- [1] S. Tüzemen, E. Gür, *Opt. Mater.* 30 (2007) 292–310.
- [2] E.M.C. Fortunato, P.M.C. Barquinha, A.C.M.B.G. Pimental, A.M.F. Gonçalves, A.J.S. Marques, L.M.N. Pereira, R.F.P. Martins, *Adv. Mater.* 17 (2005) 590–594.
- [3] R. Martins, E. Fortunato, P. Nunes, I. Ferreira, A. Marques, M. Bender, N. Katsarakis, V. Cimalla, G. Kiriakidis, *J. Appl. Phys.* 96 (2004) 1398–1408.
- [4] T. Thundat, *Nat. Nanotechnol.* 3 (2008) 133–134.
- [5] Q.-B. Ma, Z.-Z. Ye, H.-P. He, L.-P. Zhu, J.-Y. Huang, Y.-Z. Zhang, B.-H. Zhao, *Scr. Mater.* 58 (2008) 21–24.
- [6] E. Ando, M. Miyazaki, *Thin Solid Films* 516 (2008) 4574–4577.
- [7] Y. Zhang, G. Du, D. Liu, X. Wang, Y. Ma, J. Wang, J. Yin, X. Yang, X. Hou, S. Yang, *J. Cryst. Growth* 243 (2002) 439–443.
- [8] R.J. Hong, X. Jiang, B. Szyszka, V. Sittinger, A. Pflug, *Appl. Surf. Sci.* 207 (2003) 341–350.
- [9] J.J. Chen, Y. Gao, F. Zeng, D.M. Li, F. Pan, *Appl. Surf. Sci.* 223 (2004) 318–329.
- [10] C.-W. Hsu, T.-C. Cheng, W.-H. Huang, J.-S. Wu, C.-C. Cheng, K.-W. Cheng, S.-C. Huang, *Thin Solid Films* 518 (2010) 1953–1957.
- [11] E. Ando, M. Miyazaki, *Thin Solid Films* 351 (1999) 308–312.
- [12] E. Ando, M. Miyazaki, *Thin Solid Films* 392 (2001) 289–293.
- [13] T. David, S. Goldsmith, R.L. Boxman, *Thin Solid Films* 447–448 (2004) 61–67.
- [14] D. Li, X. Fang, Z. Deng, W. Dong, R. Tao, S. Zhou, J. Wang, T. Wang, Y. Zhao, X. Zhu, *J. Alloys Compd.* 486 (2009) 462–467.
- [15] T. Ashida, K. Kato, H. Omoto, A. Takamatsu, *Jpn. J. Appl. Phys.* 49 (2010), 065501-1-4.
- [16] P.T. Hsieh, Y.C. Chen, K.S. Kao, C.M. Wang, *Appl. Phys. A: Mater.* 90 (2008) 317–321.
- [17] E.M. Bachari, G. Baud, S. Ben Amor, M. Jacquet, *Thin Solid Films* 348 (1999) 165–172.
- [18] L.-W. Lai, C.-T. Lee, *Mater. Chem. Phys.* 110 (2008) 393–396.
- [19] J.-H. Jo, T.-B. Hur, J.-S. Kwak, D.-Y. Kwon, Y.-H. Hwang, H.-K. Kim, *J. Korean Phys. Soc.* 47 (2005) S300–S303.
- [20] J. Lu, Z. Ye, J. Huang, L. Wang, B. Zhao, *Appl. Surf. Sci.* 207 (2003) 295–299.
- [21] Y.-S. Chang, J.-M. Ting, *Thin Solid Films* 398–399 (2001) 29–34.
- [22] I.-T. Tang, Y.C. Wang, W.C. Hwang, C.C. Hwang, N.C. Wu, M.-P. Hwang, Y.-H. Wang, *J. Cryst. Growth* 252 (2003) 190–198.
- [23] R.-C. Chang, S.-Y. Chu, C.-S. Hong, Y.-T. Chuang, *Surf. Coat. Technol.* 200 (2006) 3235–3240.
- [24] C.R. Aita, A.J. Purdes, R.J. Lad, P.D. Funkenbusch, *J. Appl. Phys.* 51 (1980) 5533–5536.
- [25] T. Nagata, A. Ashida, N. Fujimura, T. Ito, *J. Appl. Phys.* 95 (2004) 3923–3927.
- [26] M. Noguchi, T. Hirao, M. Shindo, K. Sakurachi, Y. Yamagata, K. Uchino, Y. Kawai, K. Muraoka, *Plasma Source Sci. Technol.* 12 (2003) 403–406.
- [27] R. Menon, K. Sreenivas, V. Gupta, *J. Appl. Phys.* 103 (2008), 094903-1-9.
- [28] Y. Kajikawa, *J. Cryst. Growth* 289 (2006) 387–394.
- [29] P. Sharma, K. Sreenivas, K.V. Rao, *J. Appl. Phys.* 93 (2003) 3963.
- [30] T. Hada, K. Wasa, S. Hayakawa, *Thin Solid Films* 7 (1971) 135.